Electron Field Emission from Carbon Nanotube Array

D. Roy Mahapatra

Overview

- Problems in biomedical X-ray generation and diagnostics
- Thermionic process vs. field emission process for X-ray generation
- Carbon nanotube based thin film, various physics involved
- An integrative multiscale approach toward modeling

  Length scale: ~1nm – 1mm
- Experiments and numerical simulations

Conventional X-Ray Production

Device Design Issues

- Cathode is a resistively heated filament (tungsten)
- Thermionic emission
- Anode target (tungsten)

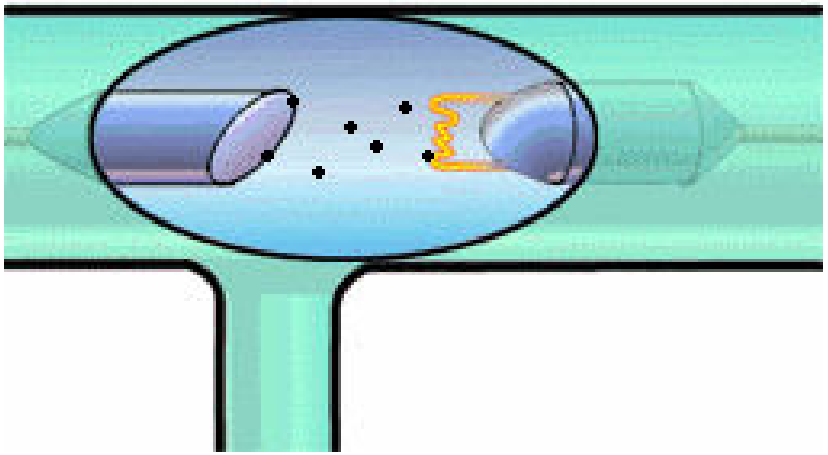

Limitations

- Poor control over beam shape for macromolecular targets
- High power consumption
- Slow response time
- Mechanical wear of the filament

Field Emission: Application of Fowler-Nordheim Model

Field Emission is an alternative to thermionic emission for electron extraction

Under a sufficiently high electric field, electrons from the Fermi level can tunnel through the potential energy barrier of a metal surface into a vacuum

Fowler-Nordheim equation was derived for field emission from a metallic surface
(Electron emission in intense electric field, R.H. Fowler and L. Nordheim, Proc. Royal Soc. A, 119, 173-181, 1928)

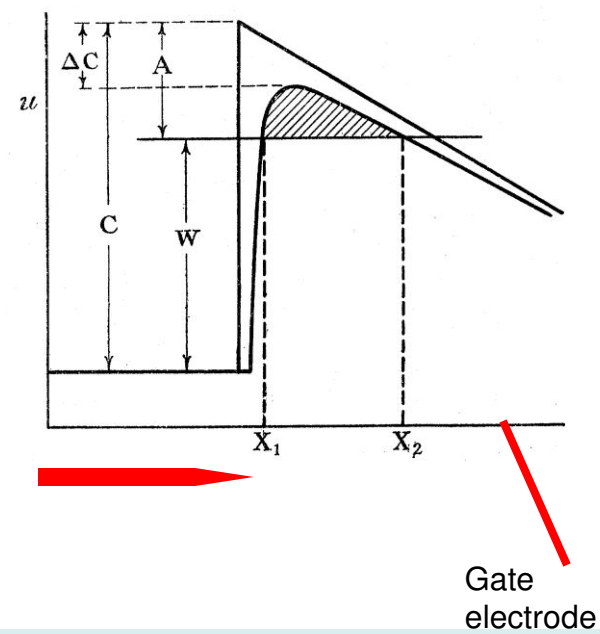

Current density: $$J = \frac{BE^2}{\Phi}\exp\left[-\frac{C\Phi^{3/2}}{E}\right]$$

$$\Rightarrow \quad \log\left(\frac{I}{V^2}\right) \quad \infty \quad \frac{1}{V}$$

Electric field E, work function Φ , B and C are constants

Field Emission: Application of Fowler-Nordheim Model

A.G. Rinzler, J.H. Hafner, P. Nikolaev, L. Lou, S.G. Kim, D. Tomanek, D. Colbert and R.E. Smalley, Unraveling nanotubes: field emission from an atomic wire, *Science*, 269, 1550-1553 (1995).

W.A. de Heer, A. Chatelain and D. Ugrate, A carbon nanotube field-emission electron source, *Science*, 270, 1179-1180 (1995).

L.A. Chernozatonskii, Y.V. Gulyaev, Z.Y. Kosakovskaya, N.I. Sinitsyn, G.V. Torgashov, Y.F. Zakharchenko, E.A. Fedorov and V.P. Valchuk, Electron field emission from nanofilament carbon films, *Chem. Phys. Lett.*, 233, 63-68 (1995).

J.M. Bonard, J.P. Salvetat, T. Stockli, L. Forro and A. Chatelain, Field emission from carbon nanotubes: perspectives for applications and clues to the emission mechanism, *Appl. Phys. A*, 69, 245-254 (1999).

H. Sugie, M. Tanemure, V. Filip, K. Iwata, K. Takahashi and F. Okuyama, Carbon nanotubes as electron source in an x-ray tube, *Appl. Phys. Lett.*, 78, 2578-2580 (2001).

Field Emission: Electronic Band Structure

- Carbon Nanotubes (CNTs) are rolled graphene sheets

- In the spirit of electron-electron and electron-phonon interactions, we calculate the electronic band structure from Hamiltonian $H(E_{\text{gap}}, \varepsilon, T, \phi, n)$

  - Lattinger-Liquid Theory (electron-electron interaction)
  - Electron-phonon interaction (frozen CNT, bare phonon calculations)
  - Charge Density Wave (CDW)

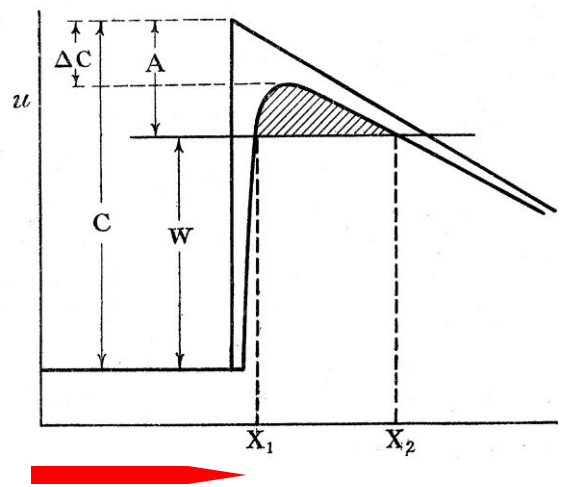

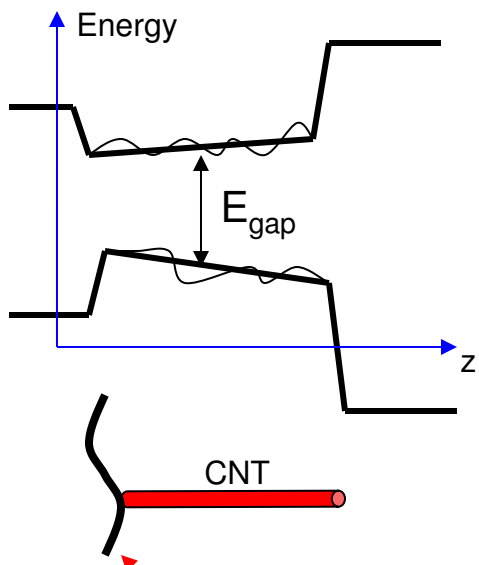

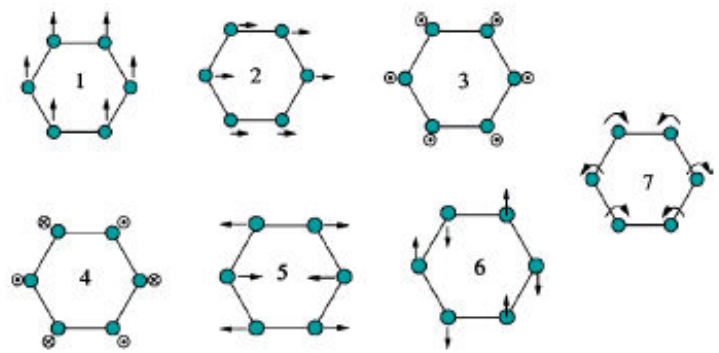

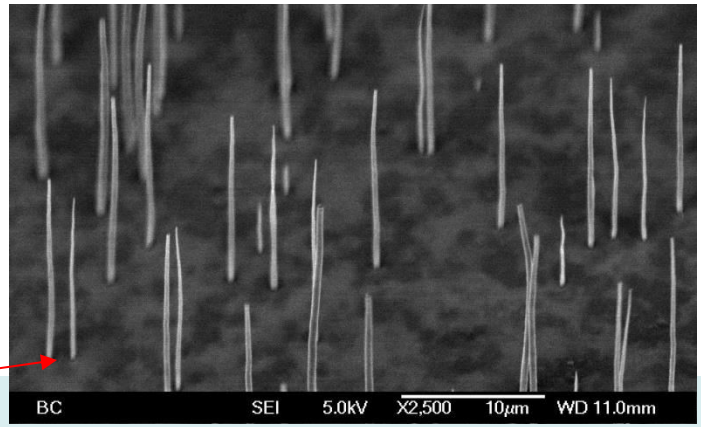

Metal-carbide

Field Emission from CNT Based Thin Films

Due to the special geometry of the CNTs vertically aligned in a thin film, a much higher current density compared to metal wire can be obtained.

Problem: CNT based thin films do not behave always as ideal metallic surfaces.

Classical analysis based on Fowler-Nordheim equation or a more accurate *k.p* + phonon calculation does not account for the following complexities:

- Evolution of the CNT thin film
  (Requires an evolution law)

- Self-assembly (reorientation) of the CNTs due to electrodynamic forcing
  (Requires an electro-mechanical model)

- Electron transport from the randomly oriented CNT tips unlike a uniform metallic surface
  (Requires a quantum-hydrodynamic type formalism)

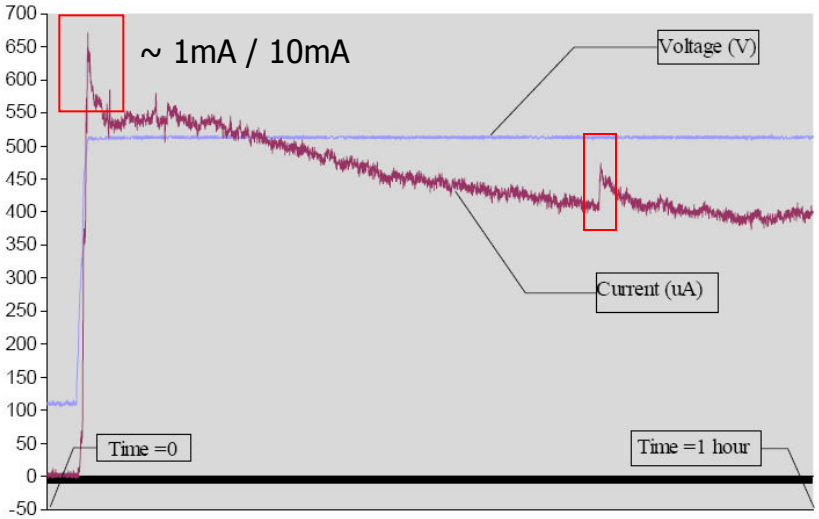

Current, Voltage-Time
Old CNT sample, Gap ≈ 250 micron, P ≈ 8.9e-7
Time is one hour

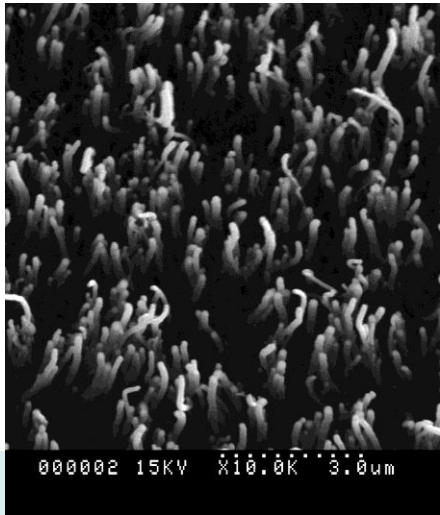

Objectives

- Experimentally, one observes frequent spiking of device current. Develop theoretical framework to understand this problem.

- In a time-resolved microscopy, one observes violent movement of the CNTs under high Electromagnetic field, often leading to damages in the film, which become visible.
  Develop numerical techniques to estimate the effects of such events.

- Perform sensitivity studies, which would be useful to understand how one can design field emission pixels for spatio-temporally controlled X-ray dosage.

Idealization of a CNT Based Thin Film

- CNTs are grown on a substrate to form a thin film.

- A representative volume element (cell) is considered in which a number of CNTs can be in arbitrarily oriented forms along with an estimated amount of carbon clusters.

- The assembly of the cells represent a thin film of planer dimension in (x,y).

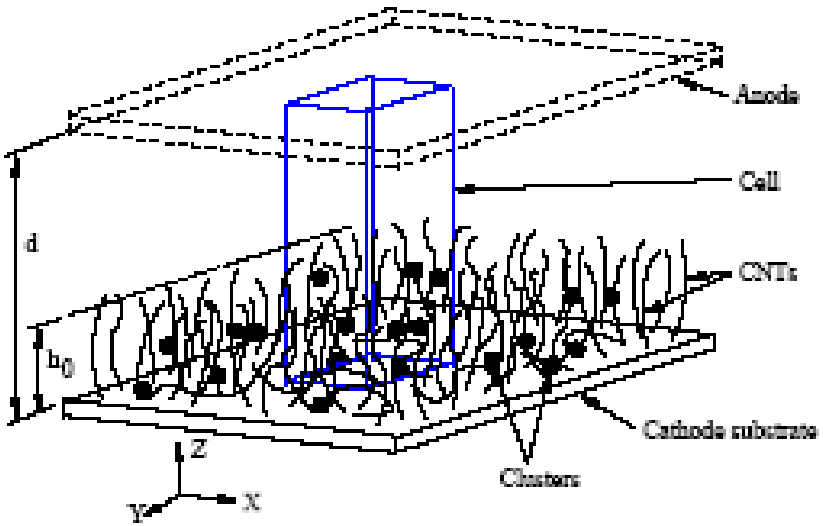

Sinha et al., J. Computational & Theoretical Nanoscience, 4 (2007) 1-15

Idealization of a CNT Based Thin Film

- Each CNT is discretized by nodes and segments along its axis.
  - A deformation in the slow scale defines the orientations of the segments.
  - A deformation in the fast scale (due to electron flow) defines the fluctuation of the rolled graphen sheet in the CNTs.
  - The combined deformation influences the electronic band structure.

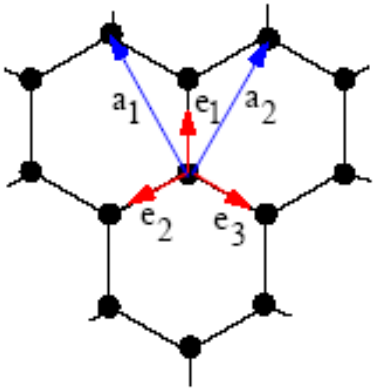

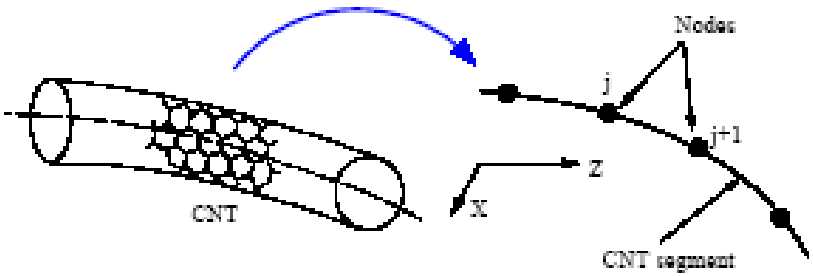

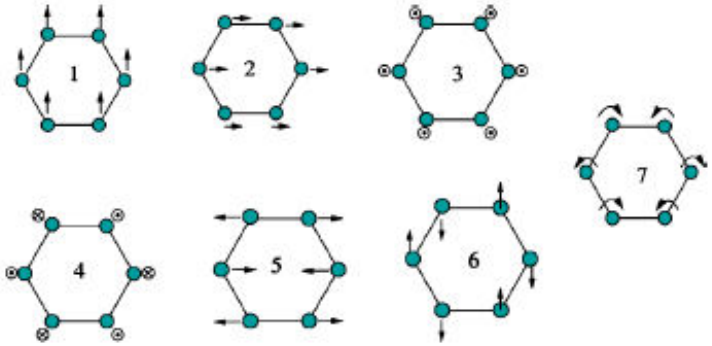

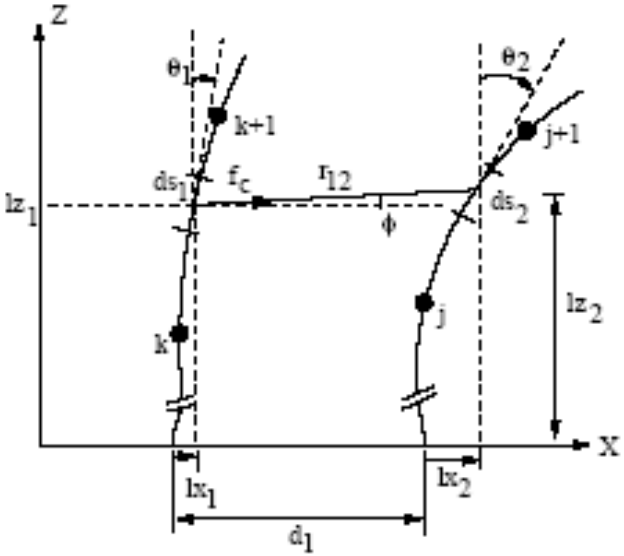

Modeling Overview

- Evolution in CNT based thin film during field emission.

- Electro-mechanical forces on the CNT array and mechanism of reorientation.

- Electron-phonon interaction.

- Systematic coupling of the evolution model, the electromechanical forcing model, momentum balance equations, and thermodynamics of electron-phonon interaction for predicting the system-level dynamics.

Degradation of CNTs: Evolution Law

$$N_{\mathrm{T}} = NN_{\mathrm{CNT}} + N_{\mathrm{cluster}} \quad \Rightarrow \quad N(t) = \frac{1}{N_{ring}\,L(t)}\left[N_{\mathrm{T}} - V_{\mathrm{cell}}\int_0^t dn_1(t)\right] \qquad \frac{dn_1}{dt} = f(T, r_{ij}, p^*)$$

A nucleation coupled treatment to the degradation of the CNT system
(Theory developed for aerosol: S.K. Friedlander, Ann. N.Y. Acad. Sci., 404, 354-364, 1983)

Ensemble average of interest: j-mer concentration (n_1), saturation ratio (S),
Total surface area of plasma (A_n), moment (M_1) of cluster size distribution

$$\frac{dN_{\mathbf{kin}}}{dt} = J_{\mathbf{kin}}$$

$$\frac{dS}{dt} = -\frac{J_{\mathbf{kin}} S g^*}{n_1} - (S-1)\frac{B_1 A_n}{2v_1}$$

$$\frac{dA_n}{dt} = \frac{J_{\mathbf{kin}} S g^{*2/3} s_1}{n_1} + \frac{2\pi B_1 S(S-1) M_1}{n_1}$$

Spatially averaged

$$\frac{dM_1}{dt} = J_{\mathbf{kin}} d_p^* + (S-1) B_1 N_{\mathbf{kin}}$$

Non-local

Degradation of CNTs: Evolution Law

$$N_{\mathbf{kin}} = \frac{n_1}{S}\exp(\Theta); \qquad S = \frac{n_1}{n_s}$$

$$g^* = \left(\frac{2}{3}\frac{\Theta}{\ln S}\right)^3; \qquad d_p^* = \frac{4\sigma v_1}{k_B T \ln S}$$

$$B_1 = 2 n_s v_1 \sqrt{\frac{k_B T}{2\pi m_1}}; \qquad \Theta = \frac{\sigma s_1}{k_B T}$$

$$M_1 = \int_{d_p^*}^{d_p^{\max}} \left(n(d_p,t) d_p\right) d(d_p)$$

$$J_{kin} = \frac{\beta_{ij} n_1^2}{12 S}\sqrt{\frac{\Theta}{2\pi}}\exp\left(\Theta - \frac{4\Theta^3}{27(\ln S)^2}\right)$$

$$\beta_{ij} = \left(\frac{3 v_1}{4\pi}\right)^{1/6}\sqrt{\frac{6 k_B T}{\rho_p}\left(\frac{1}{i}+\frac{1}{j}\right)}\left(i^{1/3}+j^{1/3}\right)^2$$

$N_{\mathbf{kin}}$: kinetic normalization constant

Θ : dimensionless surface tension

n_s : equilibrium saturation concentration of carbon cluster

g^* : critical cluster size

d_p^* : diameter of particle of critical cluster

σ : surface tension

v_1 : monomer volume

m_1 : mass of monomer

s_1 : surface area of monomer

$d_p^{\max}$: maximum diameter of the cluster

d_p : diameter of the cluster

$n(d_p,t)$: cluster size distribution function

$J_{\mathbf{kin}}$: kinetic nucleation rate

β_{ij} : collision frequency function

ρ_p : particle mass density

Degradation of CNTs: Evolution Law

Total number of CNTs in the cell:

$$N(t) = \frac{1}{N_{\mathbf{ring}} L(t)} \left[N_{\mathbf{T}} - V_{\mathbf{cell}} \int_0^t dn_1(t) \right]$$

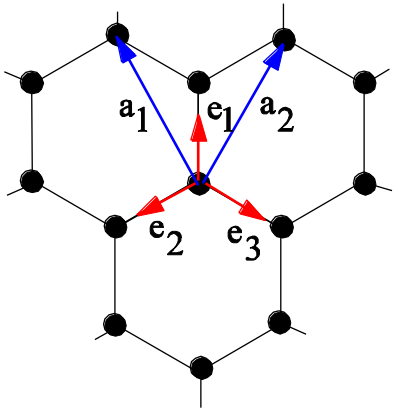

Geometry:

$$\vec{C}_h = n\vec{a}_1 + m\vec{a}_2$$

$$\vec{a}_1.\vec{a}_1 = a_1^2; \qquad \vec{a}_2.\vec{a}_2 = a_2^2; \qquad 2\vec{a}_1.\vec{a}_2 = a_1^2 + a_2^2 - a_3^2$$

$$|\vec{C}_h| = \pi d_t = \sqrt{n^2 a_1^2 + m^2 a_2^2 + nm\left(a_1^2 + a_2^2 - a_3^2\right)}$$

Decay rate for the cell:

$$v_{\mathbf{burn}} = V_{\mathbf{cell}} \frac{dn_1(t)}{dt} \left[\frac{s(s-a_1)(s-a_2)(s-a_3)}{n^2 a_1^2 + m^2 a_2^2 + nm\left(a_1^2 + a_2^2 - a_3^2\right)} \right]^{1/2}$$

$N_{\mathbf{T}}$: total number of carbon atoms

$N_{\mathbf{ring}}$: number of carbon atoms per unit length of CNT

$V_{\mathbf{cell}}$: volume of (computational) cell

(n, m) : chirality

a_1, a_2, a_3 : lattice constants

d_t : diameter of the CNT

$$s = \frac{1}{2}(a_1 + a_2 + a_3)$$

Field Emission Current Calculation

Electric field at the tip:

$$E_{z'} = \sqrt{1 - \frac{x^2 + y^2}{R^2}} \frac{(h_0 - v_{\mathbf{burn}} t) E_0}{(d - h_0 + v_{\mathbf{burn}} t)}$$

$$E_z = E_{z'} \cos\theta(t)$$

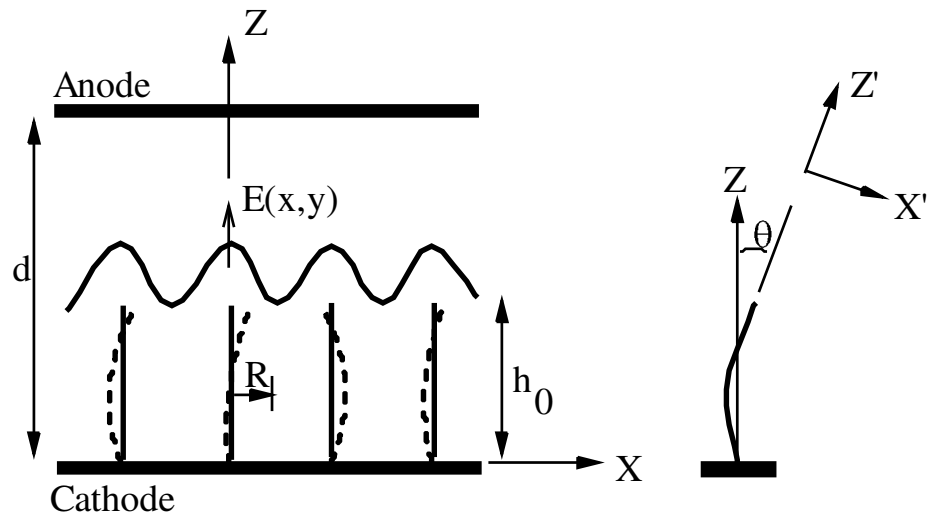

Current density (F-N Equation):

$$J(x, y) = \frac{B E_z^2}{\Phi} \exp\left[-\frac{C \Phi^{3/2}}{E_z} \right]$$

Published results based on single CNT in controlled environment:

The constants B, C, and the work function have been found to vary widely as some function of geometry, bias field, free/supported condition and alignment.

Electromechanical Forces on CNTs

- As the charge flows on the surface of CNTs, the CNTs experience Lorentz force under the influence of electric field

  (Slepyan *et al.*, Phys. Rev. B, 60, 17136-17149, 1999)

- Ponderomotive force, which act on free charges on the surface of CNTs, tend to stretch the bent CNTs. This affects the current density emitted from the tip

  (Glokhova *et al.*, Appl. Surf. Sci., 215, 149-159, 2003)

- Due to the charge on the surface of CNTs, there is an electrostatic interaction among the neighboring CNTs

- Due to van der Waals force, the cylindrical symmetry of CNTs is destroyed, which may significantly affect the electronic properties of CNTs

  (Ruoff *et al.*, Nature, 364, 514-516, 1993)

Modeling Overview

- Evolution of the CNT based thin film during field emission.
- Electromechanical forces on the CNT array and mechanism of reorientation.
- Electron-phonon interaction.
- Systematic coupling of the evolution model, the electromechanical forcing model, momentum balance equations, and thermodynamics of electron-phonon interaction for predicting the system-level dynamics.

Electromechanical Forces on CNTs

$$V_c = -eV_s - e(V_d - V_s)\frac{z}{d} + \sum_j G(i,j)(\hat{n}_j - n)$$

$$E_z = -\frac{1}{e}\frac{dV_c}{dz}$$

Lorentz force:

$$f_{lz} = \pi d_t e \hat{n} E_z \qquad f_{lx} = \pi d_t e \hat{n} E_x \approx 0$$

$$\hat{n} = \hat{n}_0 + \hat{n}_1 \begin{cases} \hat{n}_0 = \dfrac{k_B T}{\pi b^2 \Delta} \\ \dot{\hat{n}}_1 + \hat{n}_0 \dfrac{\partial \dot{u}_{z'}}{\partial z'} = 0 \end{cases}$$

(Quantum-hydrodynamic equation of continuity)

Ponderomotive force:

$$f_{pz} \approx \frac{q^2}{2m_e \omega^2} E_z \frac{\partial E_z}{\partial z} \qquad f_{px} \approx 0$$

e : electronic charge (positive)

$\hat{n}$: surface electron density

$\hat{n}_0$: steady surface electron density

$\hat{n}_1$: fluctuating surface electron density

b : interatomic distance

Δ : overlap integral(~ 2eV)

q : total charge on an elemental segment

$u_{z'}$: longitudinal displacement

m_e : mass of an electron

$$\omega = \frac{2\pi}{\tau}$$

τ : relaxation time

Electromechanical Forces on CNTs

Electrostatic force:

$$f_{cz} = \frac{1}{4\pi\varepsilon\varepsilon_0}\int_0^{s_2}\frac{(\pi e\hat{n}_0)d_t^{(1)}d_t^{(2)}}{r_{12}^2}\sin\phi ds_2$$

$$f_{cx} = \frac{1}{4\pi\varepsilon\varepsilon_0}\int_0^{s_2}\frac{(\pi e\hat{n}_0)d_t^{(1)}d_t^{(2)}}{r_{12}^2}\cos\phi ds_2$$

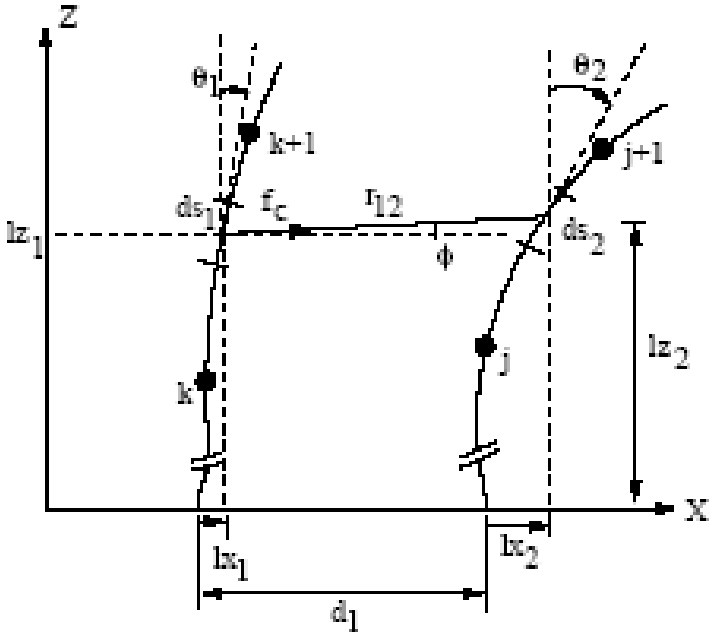

van der Waals force:

$$u_{z'}^{(m)} = u_{z'0}^{(m)} - r^{(m)}\frac{\partial u_{x'}^{(m)}}{\partial z'}$$ (Euler-Bernoulli beam)

$$f_{vs} = \sum_m \pi C_{vs}\left[\left(r^{(m+1)}\right)^2 - \left(r^{(m)}\right)^2\right]\frac{1}{\Delta_{x'}}\frac{\partial \Delta_{x'}}{\partial z'}$$ (MNT)

$$f_{vs_z} = f_{vs}\sin\theta(t); \qquad f_{vs_x} = f_{vs}\cos\theta(t)$$

ε : effective permittivity

ε_0 : permittivity of free space

$d_t^{(1)}, d_t^{(2)}$: diameters of two neighboring CNTs

m : wall number of the CNT

$u_{z'0}^{(m)}$: longitudinal displacement of the centre of the cross-section

C_{vs} : van der Waals coefficient

Dynamics of CNTs: Momentum Balance Equations

Net force components:

$$f_z = \int \left(f_{lz} + f_{vs_z} \right) ds + f_{cz} + f_{pz}$$

$$f_x = \int \left(f_{lx} + f_{vs_x} \right) ds + f_{cx} + f_{px}$$

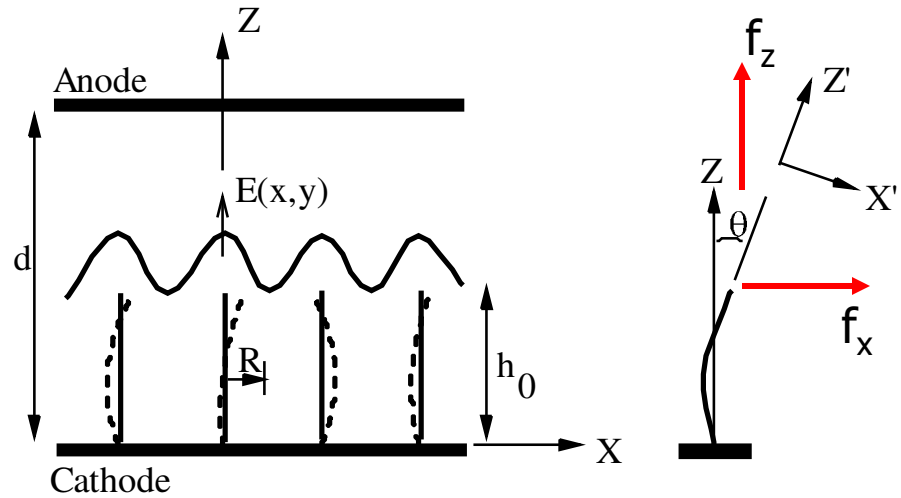

In the governing equations of motion, CNTs are treated as 1D nonlinear elastic wires.

$$-E' A_0 \frac{\partial^2 u_{z'0}^{(m)}}{\partial z'^2} - \frac{1}{2} E' A_0 \alpha \frac{\partial \Delta T(z')}{\partial z'} + \rho A_0 \ddot{u}_{z'0}^{(m)} - f_{vs_{z'}} - f_{lz'} - f_{cz'} = 0$$

$$E' A_2 \frac{\partial^4 u_{x'}^{(m)}}{\partial z'^4} + \rho A_0 \ddot{u}_{x'}^{(m)} - \rho A_2 \frac{\partial^2 \ddot{u}_{x'}^{(m)}}{\partial z'^2} - f_{vs_{x'}} - f_{lx'} - f_{cx'} = 0$$

A_0 : effective cross-sectional area

A_2 : second area moment

ρ : mass per unit length

Modeling Overview

- Evolution of the CNT based thin film during field emission.
- Electromechanical forces on the CNT array and mechanism of reorientation.
- Electron-phonon interaction.
- Systematic coupling of the evolution model, the electromechanical forcing model, momentum balance equations, and thermodynamics of electron-phonon interaction for predicting the system-level dynamics.

Thermodynamics of Electron-Phonon Interaction

Heat generated due to the conduction electron emitted from the CNT tips produces phonons

$$dQ = I^2 \frac{\rho_C \pi d_t^2}{4L} dz'$$

$$dQ - \frac{\pi d_t^2}{4} dq_F - \pi d_t \sigma_{SB}\left(T^4 - T_0^4\right) dz' = \beta_{in} k_B \frac{\partial T}{\partial t}$$

Temperature dependent conductance $k_Q = \pi k_B^2 T/(6\hbar)$

(Chiu *et al.*, Phys. Rev. Lett. **95**, 226101 (2005))

Boundary conditions: $z = 0, \quad T = T_0$

$$z = L(t), \quad q_F \propto k_Q T^2 \frac{d_t^2}{a_1 c}$$

dQ : heat flux

I : current

ρ_C : electrical resistivity

L : effective length of CNT

q_F : Fourier heat conduction

σ_{SB} : Stefan-Boltzmann constant

Coupled Model

$$\frac{\partial^2 \hat{n}_1}{\partial t^2} - \frac{e\hat{n}_0}{m_e}\frac{\partial E_{z'}}{\partial z'} - \alpha_L \frac{\partial^2 \hat{n}_1}{\partial z'^2} + \beta_L \frac{\partial^4 \hat{n}_1}{\partial z'^4} + \frac{\beta_L}{r^2}\frac{\partial^4 \hat{n}_1}{\partial z'^2 \partial \theta_0^2} + \frac{n_0}{m_e}\frac{\partial f_{lz'}}{\partial z'} - \frac{e\hat{n}_0}{m_e}\frac{1}{r}\frac{\partial E_{\theta_0}}{\partial \theta_0} - \frac{\alpha_L}{r^2}\frac{\partial^2 \hat{n}_1}{\partial \theta_0^2} + \ldots = 0$$

$$\nabla^2 \mathbf{E} - \mu\sigma\frac{\partial \mathbf{E}}{\partial t} - \mu\varepsilon\frac{\partial^2 \mathbf{E}}{\partial t^2} = \mu\frac{\partial \mathbf{J}}{\partial t}, \qquad \mathbf{E} = -\nabla\phi$$

$$\hat{n}_{\mathrm{av}}^{\mathrm{CNT}} = \sum_{i=1}^{R} f_i(E_{\mathrm{FL}}, E_i^{\mathrm{band}}, T)\,|\Psi_i|^2$$

$$H(\varepsilon, T, \phi, n)\Psi = i\hbar\frac{\partial}{\partial t}\Psi$$

$$\varepsilon_{zz} \approx \frac{\Delta a_1 \sin(\alpha/2) + 0.5 a_1 \cos(\alpha/2)\Delta\alpha}{a_1 \sin(\alpha/2)}$$

Coupled model

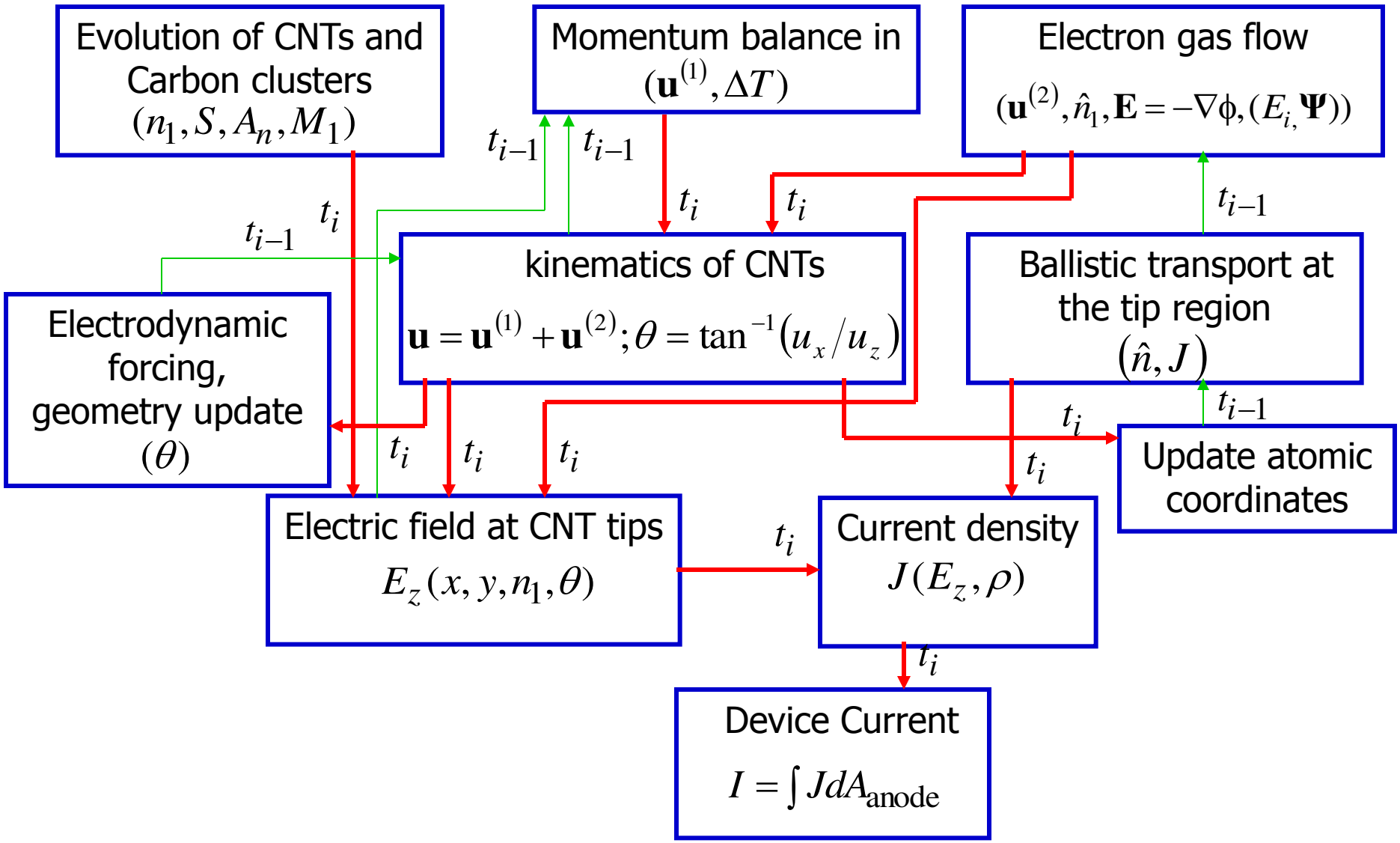

A Comparison between Simulation and Experiments

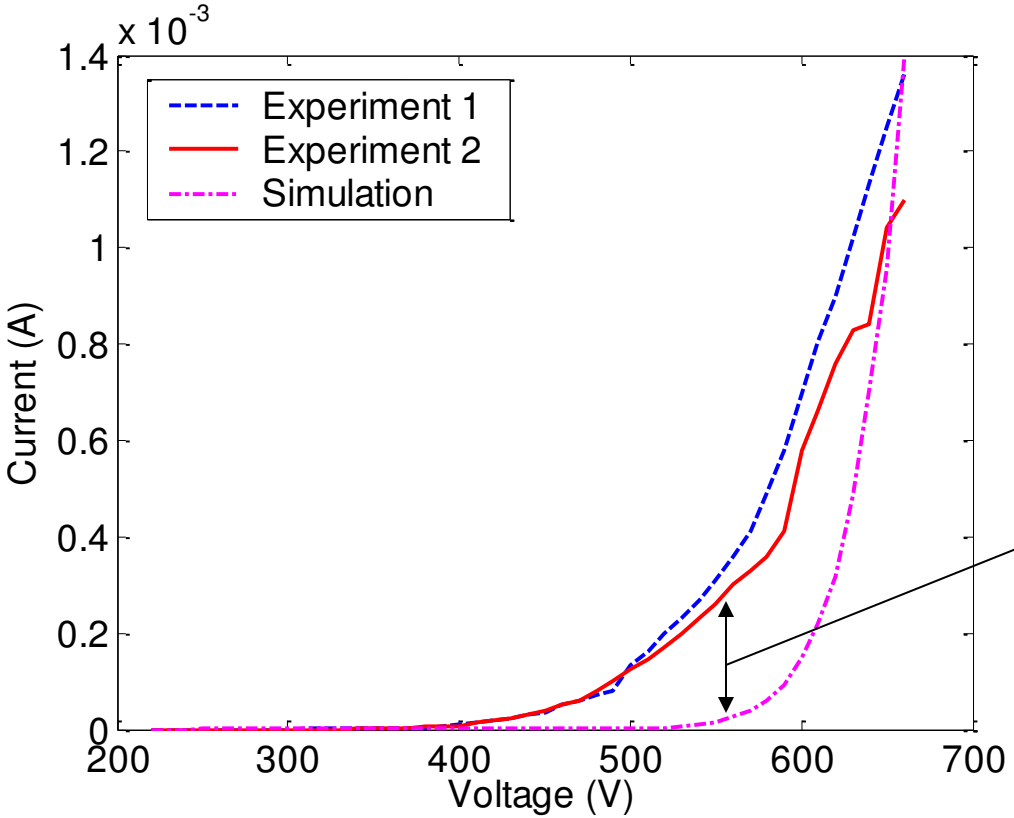

Differences due to impurities, defects, metal-carbide barrier and inhomogeneous distribution of CNT densities

Materials: CNTs grown on stainless steel substrate (Zhu *et al.*, NCSU)

Geometry: film area 49.93 mm^2,

Average height of CNTs = 12 μm

Average diameter of CNTs = 3.92 nm

Average CNT space at substrate = 2 μm

Electrode gap = 34.7 μm

Numerical Simulation: Carbon Cluster Concentration

Reduction of number of carbon molecules from CNTs over time

Initial condition: $S(0)=100$, $T=303$ K, $M_1(0)=2.12 \times 10^{-16}$, $A_n(0)=0$

- For $n_1(0)=100$ and 150, the rate of decay is very slow

- For $n_1(0)=500$, CNTs decay comparatively faster (but still insignificant) for first 34 seconds

- It can be concluded that the rate of decay is very slow, which implies longer lifetime of the cathode

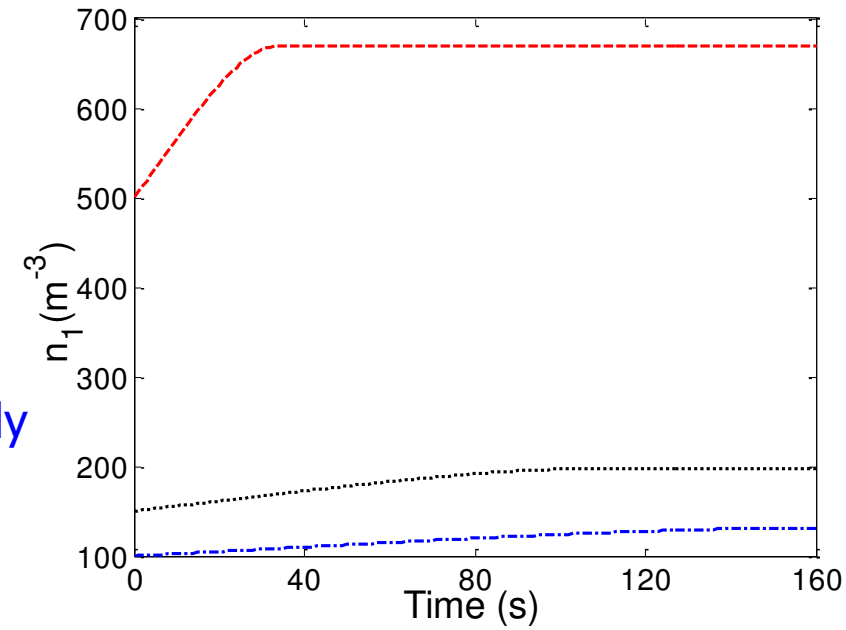

Variation of carbon cluster with time at three different values of $n_1(0)$

Numerical Simulation: Carbon Cluster Concentration

Effect of S(0) on carbon cluster concentration

Initial condition: $n_1(0)=100\ m^{-3}$, T=303 K, $M_1(0)=2.12 \times 10\text{-}16$, $A_n(0)=0$

- For S(0)=50, decay is not observed for a small time interval

- For S(0)=150, CNTs decay comparatively faster for the period of 160 seconds compared to the other two cases

- It can be concluded that a smaller value of S(0) is favorable for longer lifetime of the cathode

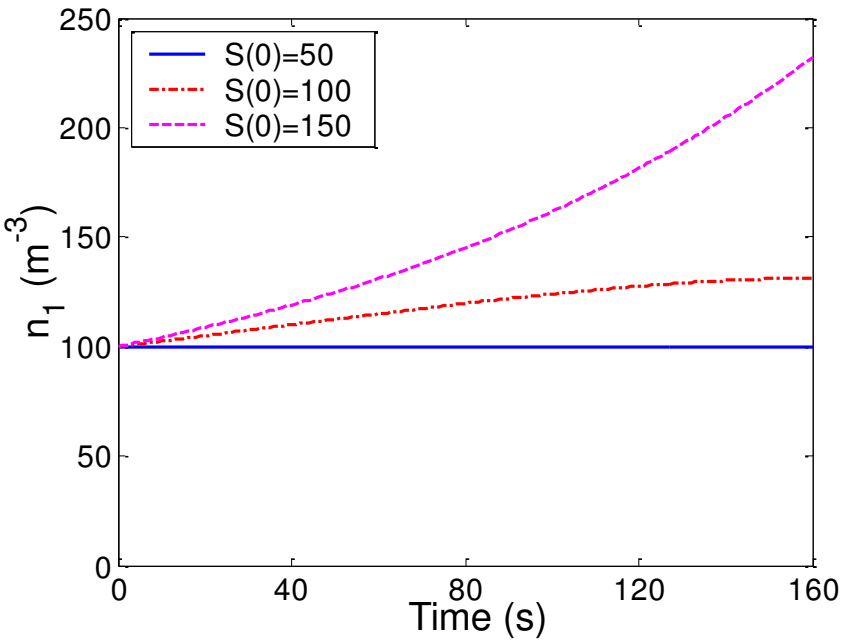

Variation of carbon cluster with time at Three different values of S(0)

Degradation

Standardless Quantitative Data

Element	Wt%	At%
C K	32.47	45.84
O K	29.11	30.86
MgK	1.11	0.77
AlK	31.14	19.57
ClK	6.18	2.96

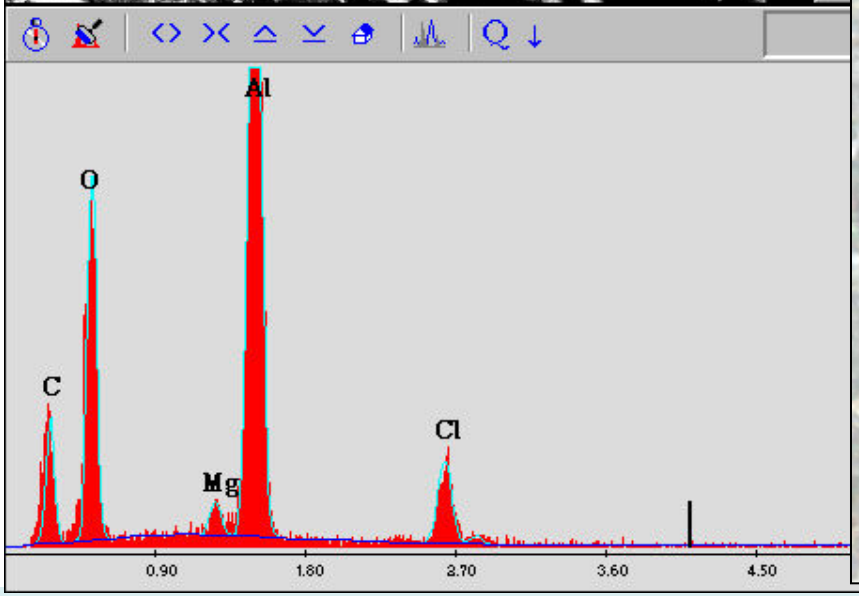

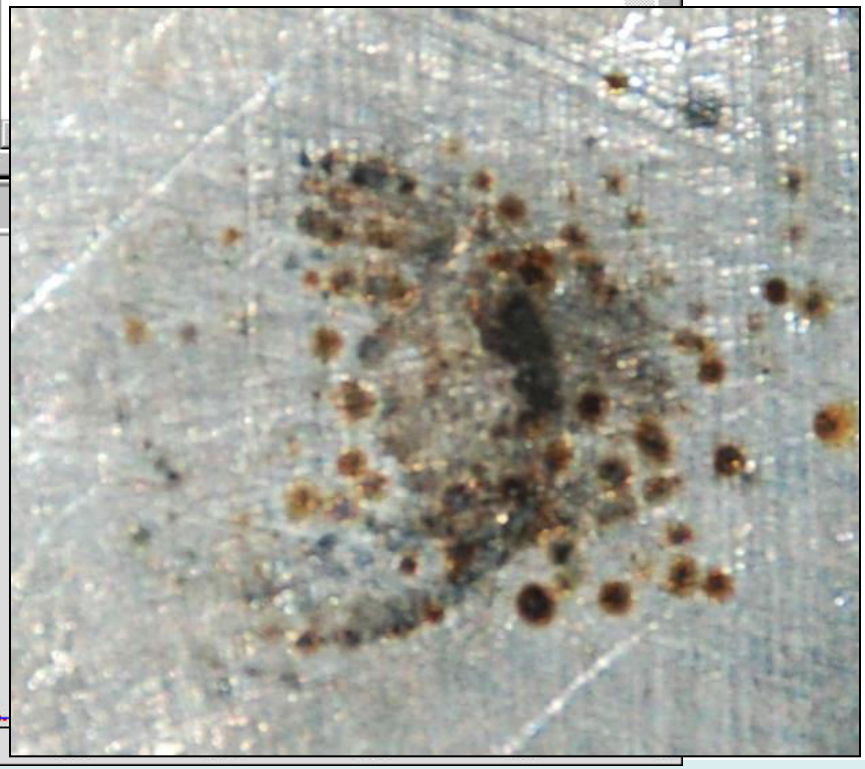

Numerical Simulation: Device Current

Field emission current for various initial average tip deflections and bias voltages :

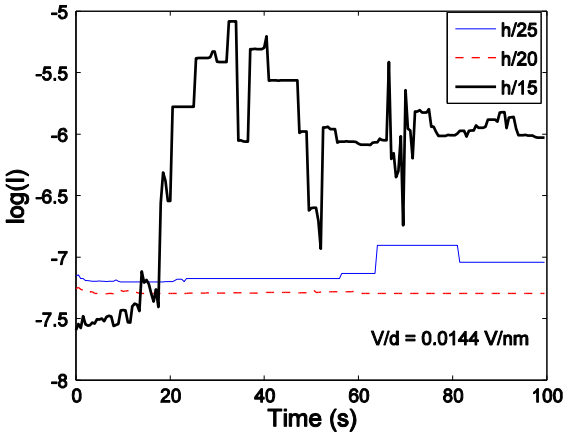

(a) V_0=500 V

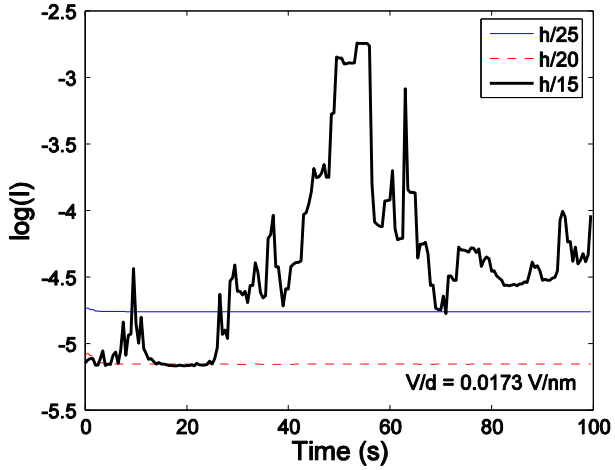

(b) V_0=600 V

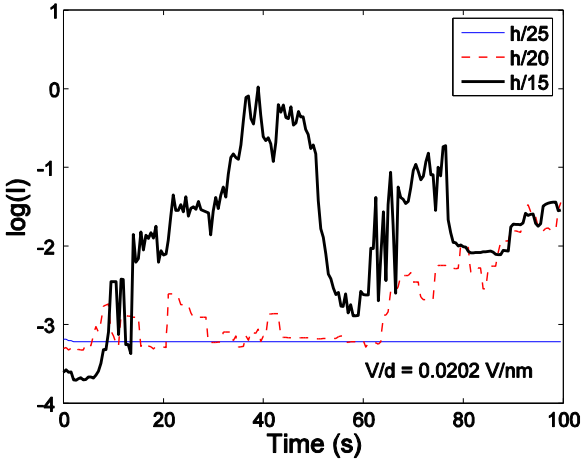

(c) V_0=700 V

- As the initial state of deflections increases, the average current reduces, until the deflection becomes large enough that there is a sudden pull due to electrodynamic forces
- At higher bias voltage, the current spike has an amplitude factor of $\sim 10^3$, whereas at lower bias voltage, the amplitude factor is $\sim 10^2$

Numerical Simulation: Visualization

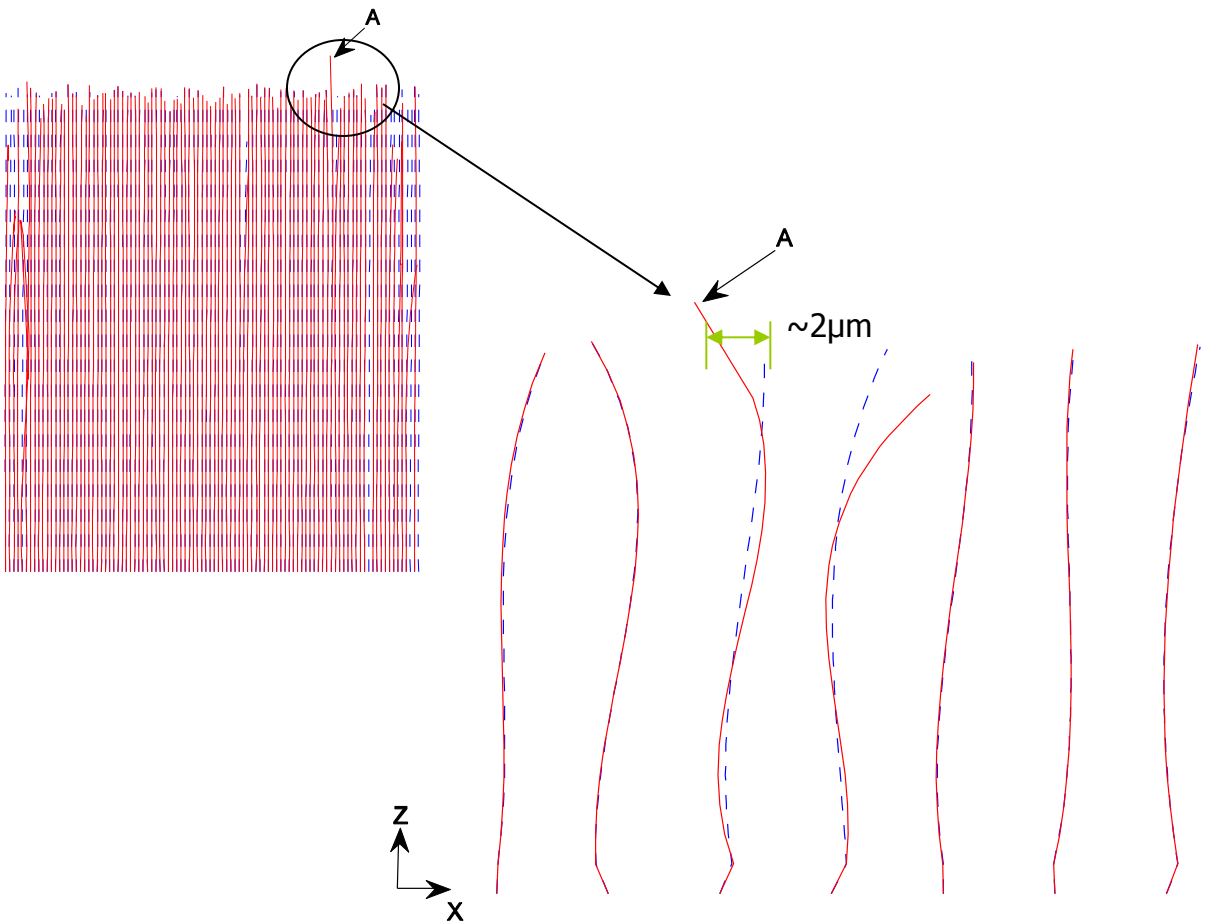

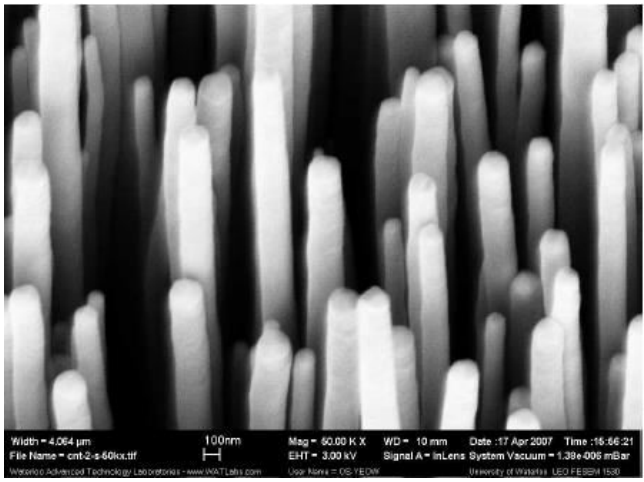

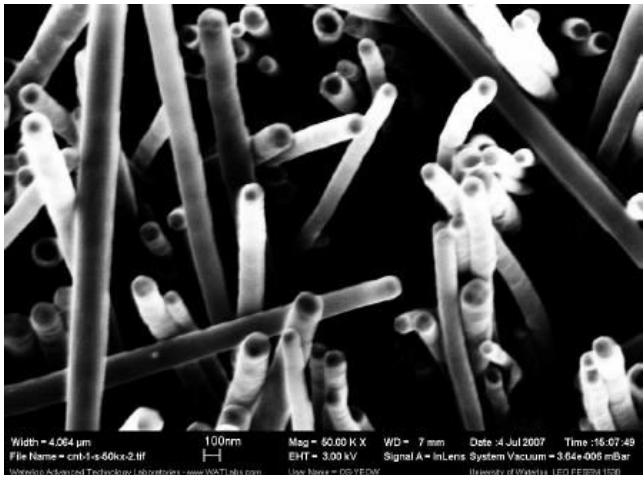

Electrodynamic stretching and reorientation of the CNTs

Sinha, Roy Mahapatra, Yeow, Melnik, Jaffray, Computational and Theoretical Nanoscience, Dec 2006; IEEE Tras. Nanotechnology 2007 (accepted), PRB 2007 (under review)

Numerical Simulation: CNT tip Orientations

Comparison of tip orientation angles at t=0 second and t=100 second for an array of 100 CNTs:

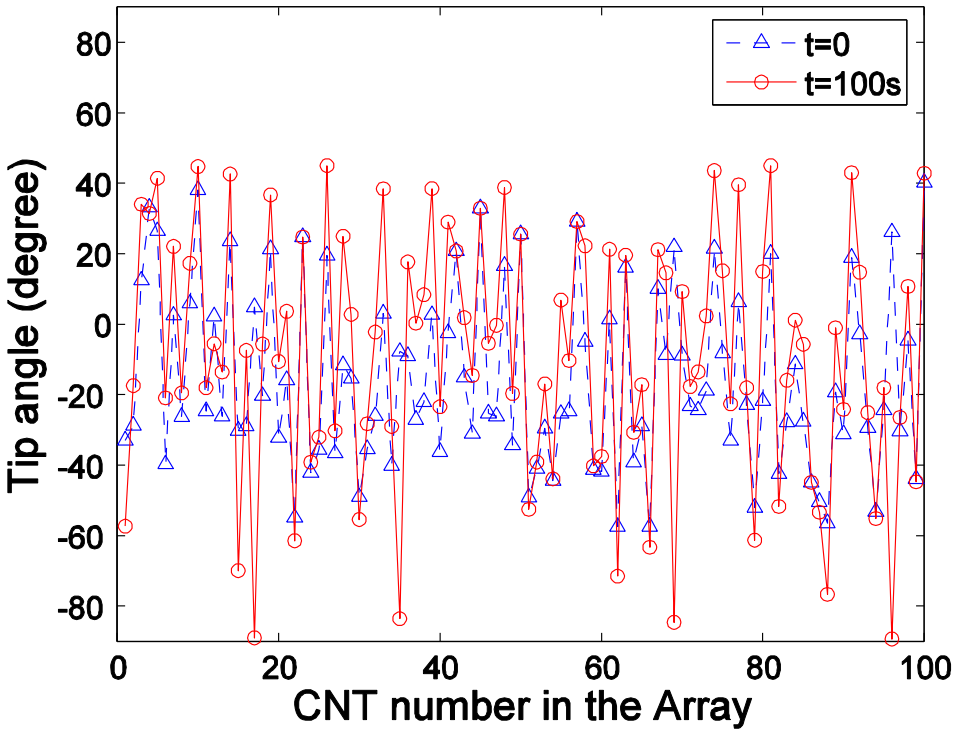

Due to electrodynamic interaction, the CNTs reorient themselves from positive to negative angles

Numerical Simulation: Tip Temperature

Maximum temperature of CNT tips during 100 seconds of field emission at a bias voltage of 700V :

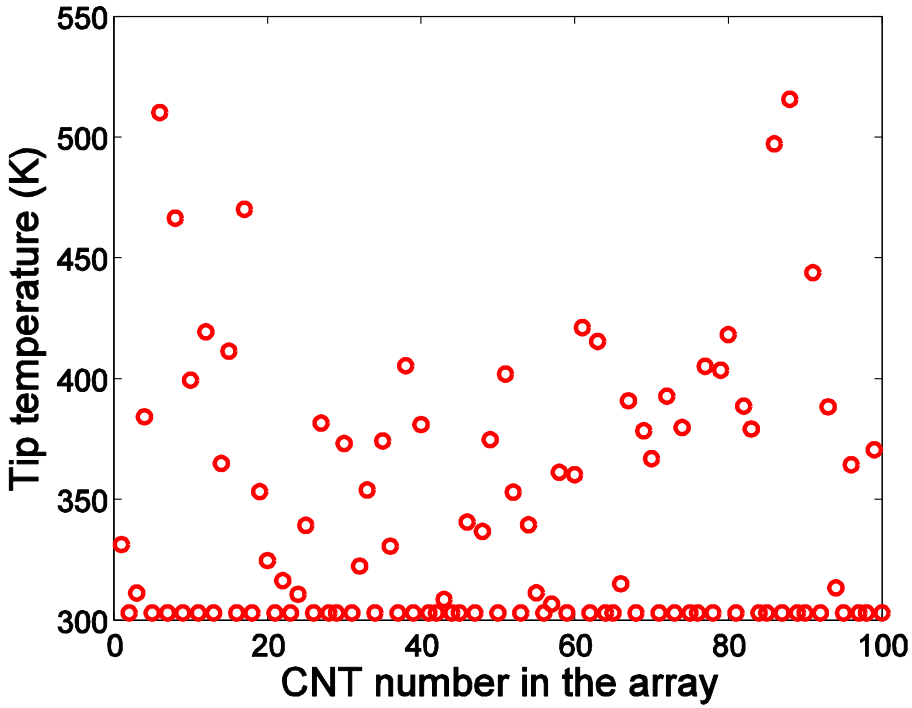

The temperature rises up to 520 K for a bias field of 0.0202 V/nm at t=40 seconds

Numerical Simulation: Current vs. Bias Field

Variation in the maximum current and the average current due to field emission under increasing bias electric field

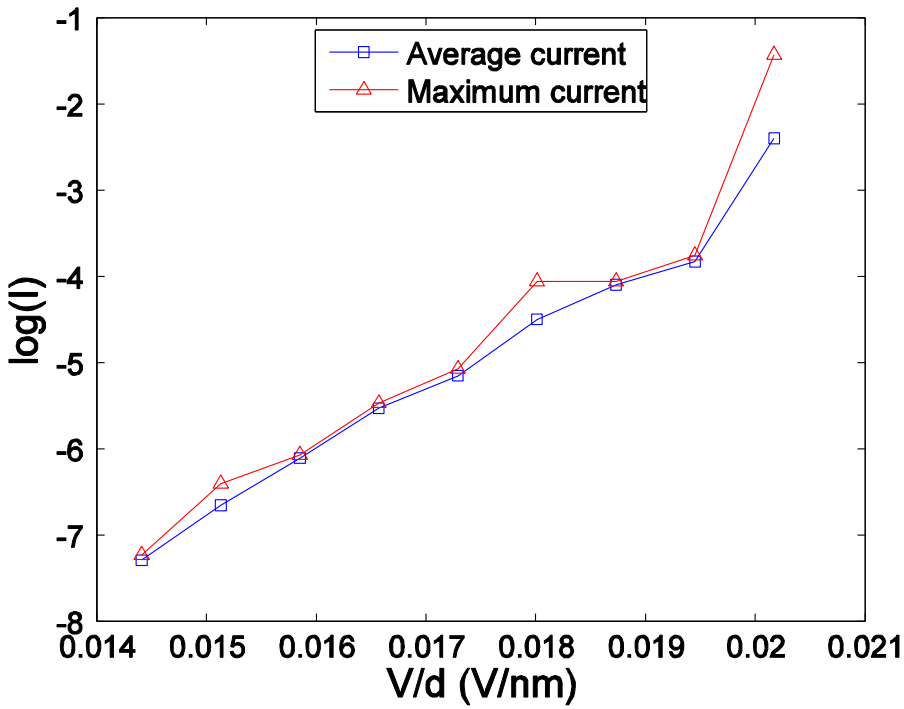

- A linear log(I) vs V/d behavior is observed initially
- At higher bias fields, the maximum current varies significantly compared to the average current

Numerical Simulation: Temperature vs. Bias Field

Variation in the maximum temperature and the average temperature due to field emission under increasing bias electric field

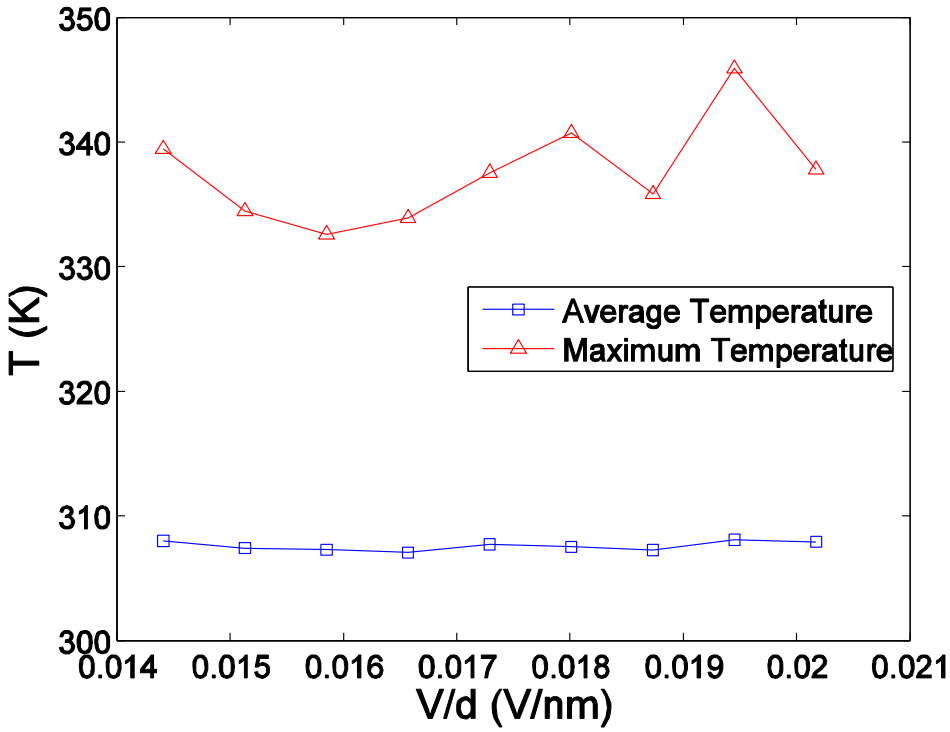

- The average temperature is almost independent of the bias field
- The maximum temperature fluctuates by 10 K

Phonon Assisted Field Emission Amplification

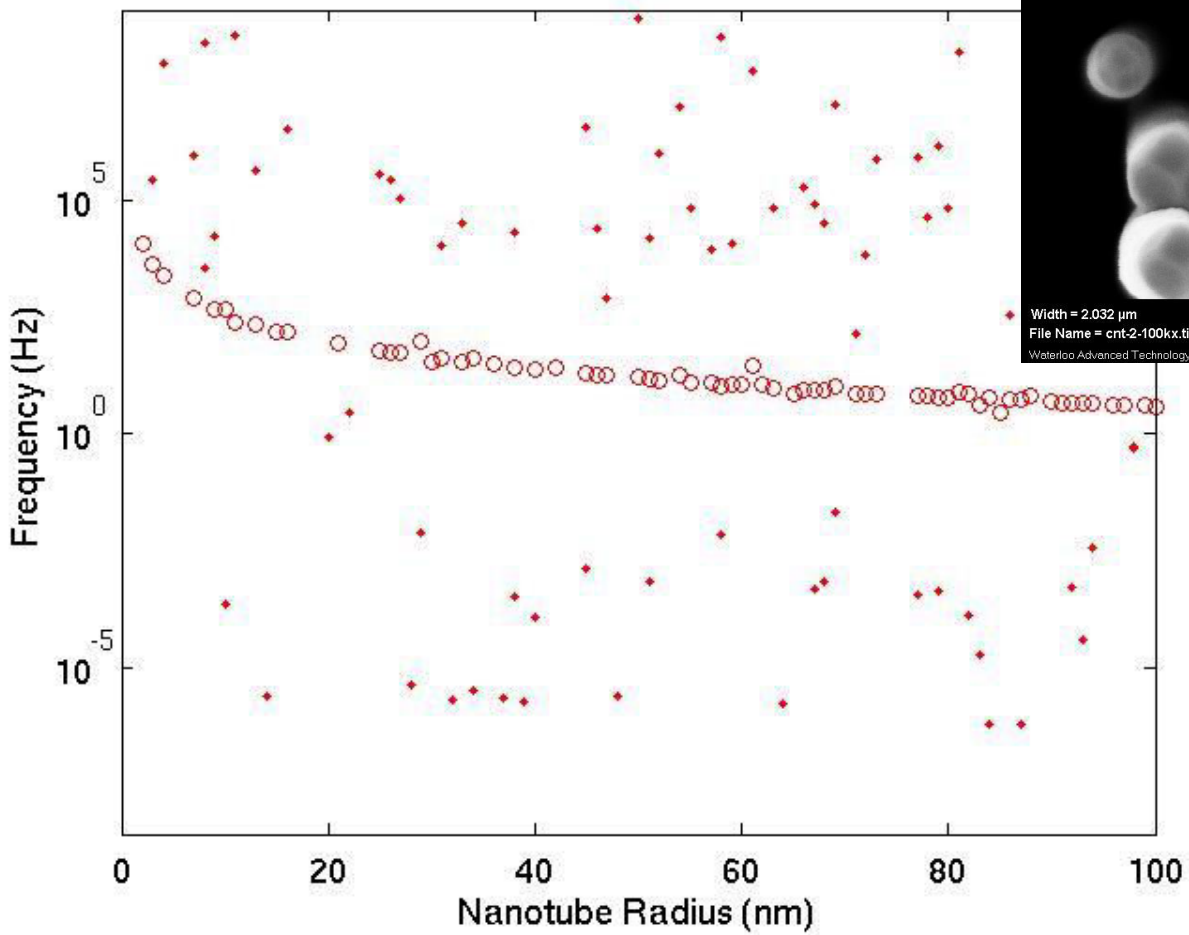

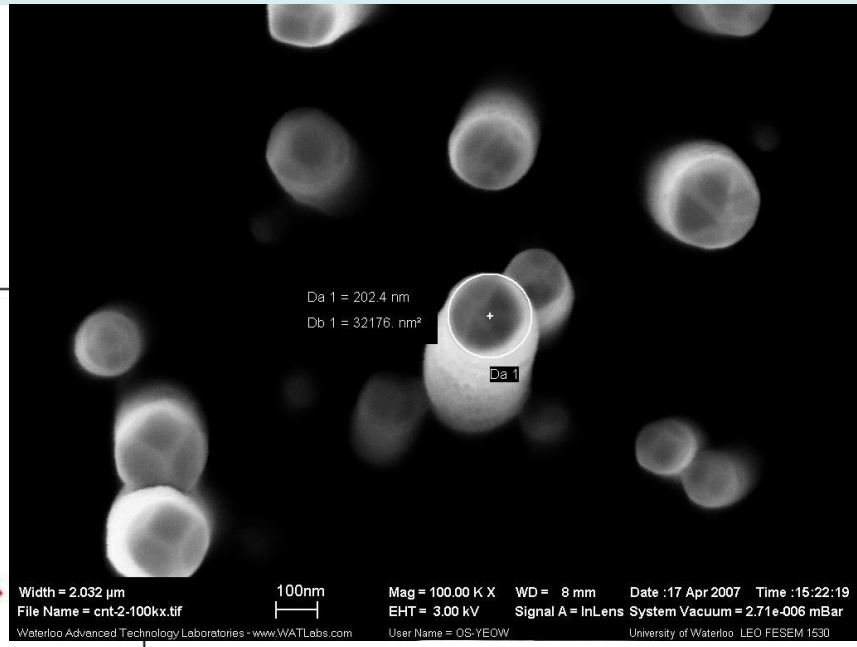

Phonon Assisted Field Emission Amplification

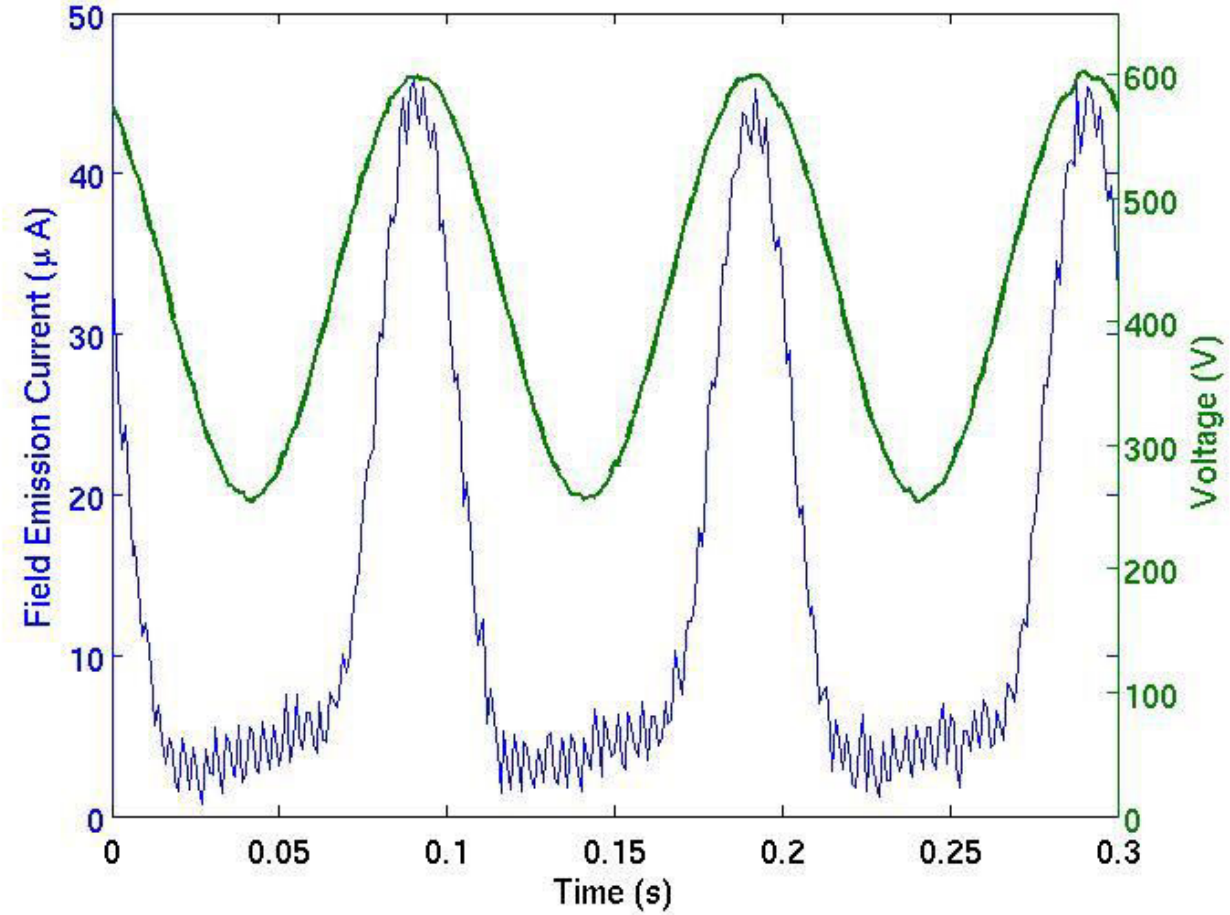

Continuous emission due to 10Hz background EM excitation

Phonon Assisted Field Emission Amplification

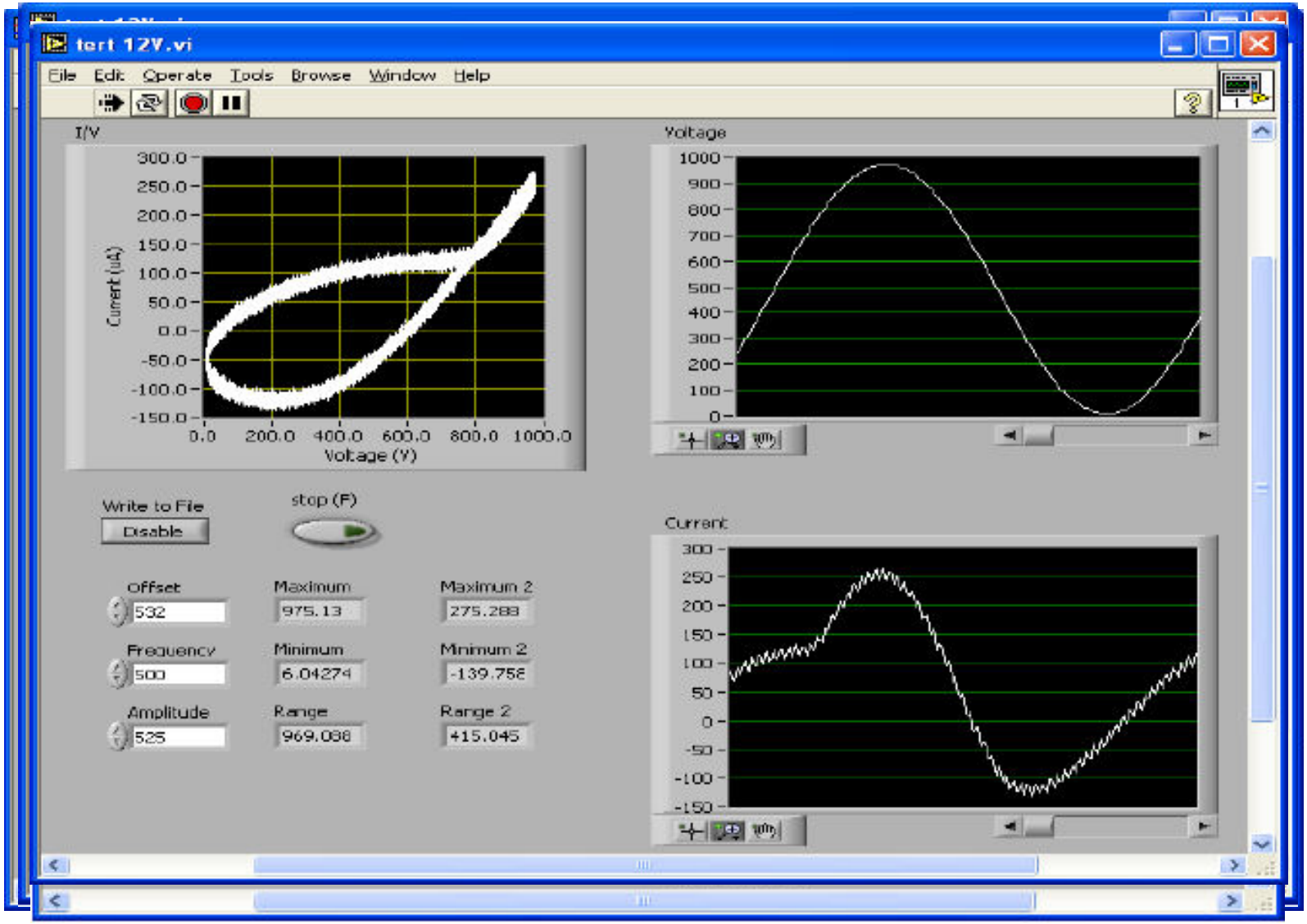

Concluding Remarks

- A coupled model has been developed, which employs a nucleation model of degradation of CNTs, the electro-mechanical forces on the randomly oriented CNTs, the mechanics of CNTs, and the thermodynamics of electron-phonon interaction.

- As the published experimental studies indicate, the device current history consists several spikes. The present simulation revels that such spikes are due to the electrodynamic pull on the CNTs and related coupled phenomena.

- While capturing the current spikes, the present simulation has also captured the intense temperature rise as observed in experiments.

- Ongoing research is to design field emission pixels for spatio-temporally controlled X-ray dosage